Manuscript Details

Manuscript number	AUTCON_2018_398_R1
Title	Assessment of Compliance of Dimensional Tolerances in Concrete Slabs using TLS data and the 2D Continuous Wavelet Transform
Article type	Original article

Abstract

While several concrete waviness assessment methods are being developed to overcome the disadvantages of one assessment method over the other, the sparseness of measurements associated with each method prevents from achieving a better understanding of how elevations and undulations change across the surface. Assessing waviness over multiple one-dimensional (1D)-survey lines may not accurately reflect the actual condition or waviness of the entire floor. The methodology presented in this paper presents a compliance-checking algorithm for detecting elements where dimensions exceed specified tolerance. It also enables assessment of a concrete surface in two-dimensional (2D) domain using the synergy of Terrestrial Laser Scanning (TLS) and Continuous Wavelet Transform (CWT). 2D CWT analysis provides information not only about the periods of the surface undulation, but also the location of such undulations. The validity of the methodology is established by running a test on point clouds obtained from a warehouse project near Gresham, Oregon. A rigorous comparison between one of the existing floor waviness measurement methods, the waviness index method, and the proposed method is made. The results showed that the proposed methodology delivers accurate results that enable the localization of surface undulations of various characteristic periods. Furthermore, the proposed method is more efficient in terms of time taken for acquiring the measurements, and is, thus, more cost efficient.

Keywords	Dimensional Quality Control; Tolerance Compliance; Terrestrial Laser Scanning; Point Cloud; Continuous Wavelet Transform; Depth Map
Corresponding Author	Yelda Turkan
Corresponding Author's Institution	Oregon State University
Order of Authors	Nisha Puri, Enrique Valero, Yelda Turkan, Frédéric Bosché
Suggested reviewers	Changwan Kim, Pingbo Tang, André Borrmann, Kevin Han, Mohammad Nahangi

Submission Files Included in this PDF

File Name [File Type]

Cover Letter_06052018.pdf [Cover Letter]

Dimensional QC using TLS Point Clouds_R1_Response to reviewers' comments.docx [Response to Reviewers]

Highlights.docx [Highlights]

Dimensional QC using TLS Point Clouds_R1.docx [Manuscript File]

To view all the submission files, including those not included in the PDF, click on the manuscript title on your EVISE Homepage, then click 'Download zip file'.

Yelda Turkan, Ph.D.
Robert C. Wilson Faculty Scholar
Assistant Professor
Construction Engineering
Oregon State University
201E Kearney Hall
Corvallis, Oregon 97331 USA

Oregon State University

Tuesday, June 05, 2018

Miroslaw J. Skibniewski, Ph.D.
Editor-in-Chief of Automation in Construction
A. James Clark Chair Professor
Department of Civil & Environmental Engineering
A. James Clark School of Engineering
Glenn L. Martin Hall 1188
University of Maryland
College Park, MD 20742, USA

Dear Professor Skibniewski,

Please find enclosed an electronic copy of the submission of "Adaptive Wavelet Neural Network for Terrestrial Laser Scanner-Based Crack Detection" by Nisha Puri, Enrique Valero, Yelda Turkan and Frédéric Bosché.

Thank you for the constructive reviews, which we felt helped us improve the paper. The manuscript has been revised according to comments made by the reviewers, received by the authors on June 4, 2018. A detailed description of the responses and changes made due to the reviewers' comments is also attached.

Should you need to contact me, please email at yelda.turkan@oregonstate.edu. Other means of contacting me include the address listed above, and by telephone at 541-737-2631.

Please let me know if there is any way that I may be of further assistance.

Sincerely,

Yelda Turkan

Yelda Turkan

Assessment of Compliance of Dimensional Tolerances in Concrete Slabs using TLS data and the 2D Continuous Wavelet Transform

Nisha Puri, Enrique Valero, Yelda Turkan, Frédéric Bosche

We appreciate the editor and reviewers' valuable comments and recommendations to improve this paper. We have revised our manuscript following each of their recommendations, which are responded in detail below. The line numbers in the third column refers to the line numbers in the revised manuscript.

Detailed Responses to the Editor and Reviewers' Comments

<u>**Editor**</u>
We appreciate the editor's comments. The following table summarizes any changes made to the manuscript as suggested by the editor.

Comments	Response – Changes Applied	Line No
This manuscript has received two comprehensive reviews, each suggesting that minor modifications be made to the paper before it can be considered for publication. The authors are encouraged to revise the manuscript and resubmit it for a new round of review as a technical paper. The specific review comments are below. Please respond point-by-point, preferably in table format, to each review comment with the location in the paper of any changes made. In the References, all cited items must include full bibliographic data and DOI (for all papers in journals and conference proceedings), ISBN (for all books) or web address with the date of last access (for all	Thank you. We have added and updated the full bibliographic data, DOI, ISBN and web addresses.	467, 468, 471-473, 550, 551, 568, 609, 610, 612, 616-622, 633-635

technical reports and misc. documents) - no exceptions. Do not abbreviate journal names or conference titles.		

Reviewer # 1

We appreciate the reviewer's comments. The following table summarizes any changes made to the manuscript as suggested by the reviewer.

Comments	Response – Changes Applied	Line No
This manuscript addresses an essential need of accurate and rapid flatness assessment of concrete slabs. Building upon previous work by the authors, this study presents a 2D CWT analysis method for analyzing laser scanned point cloud data. This manuscript is well written and properly organised. The reviewer believes this manuscript is suitable for publication after addressing the following comments and minor errors.	Thank you.	
1) Lines 85 and 329: please correct the reference link errors.	We have corrected the reference link errors.	85, 333
2) Line 342: It is assumed this figure is a mistaken insert?	Thank you for pointing it out. We have removed it.	345
3) Figure 7: reorganise the figures so they fit nicely and have the same font sizes (7(e) apparently has bigger fonts).	Thank you for the suggestion. We have reorganized the figures.	360

Reviewer # 2

We appreciate the reviewer's comments. The following table summarizes any changes made to the manuscript as suggested by the reviewer.

Comments	Response – Changes Applied	Line No
1) Overall, this paper is well structured and presented. The proposed methods are clear and technically satisfactory. Evaluation is well organized and supports validity of the proposed method. However, one major concern is that the methodological similarity with the previous papers, such as Bosche and Biotteau (2015) and Bosche et al. (2014), seems to be high. The authors need to clarify the originality of this paper compared to the authors' previous studies.	Thank you. The work presented here is significantly different than those two papers. Please see below detailed explanations on the differences between those studies and the one presented here: - The work presented in **Bosché and Guenet (2014)** digitally applied two traditional methods of measuring floor flatness (F-number and Straightedge) to 1D survey lines derived from TLS data, and does not consider at all using a different approach like Continuous Wavelet Transform (CWT) that is proposed here. In contrast, we apply our approach to the entire 2D surface derived from TLS data, as opposed to 1D survey lines derived from TLS data. And, our study overcomes the issue of spatial resolution and enables the analysis of surface undulations of all periods, owing to the innovative application of the Continuous Wavelet Transform. - Our methodology differs significantly from **Bosché and Biotteau (2015)** as we addressed the issue of spatial resolution in this study. The methodology we presented in this study involves the generation of floor flatness information for the entire 2D surface using Continuous Wavelet Transform (CWT). The application of 2D CWT necessitated the development of a depth map, which was not relevant to the methodology presented in Bosché and Biotteau (2015). For instance, the processes involved in the generation of depth map, such as interpolation used in obtaining z-values at each grid point, are not relevant to Bosché and Biotteau (2015).	148 – 151, 155 – 157

Bosché and Biotteau (2015) introduce the use of the CWT technique to conduct flatness control in construction. However, they do this only along 1D survey lines derived from TLS data, just like traditional methods do. Again, a significant contribution of the proposed work is to move away from the traditional approaches of working in 1D, and work fully in 2D (floors are 2D structures, and so should be treated as such). This work thus uniquely introduces the use of the CWT technique in 2D, which requires a specific approach, for example with the establishment of a 2D depth map.

In contrast to the two works above, it is also worth highlighting that the work presented here is validated using data from a fresh concrete slab that is much larger than the one used by those authors.

We have added further clarification to lines 148 through 151, and lines 154 through 155.

Highlights

> 2D CWT is applied to TLS data for floor flatness control assessment.

> 2D CWT gives information about the periods and the location of the floor undulations.

> The proposed method generates results that supersede those obtained using the WI method.

Assessment of Compliance of Dimensional Tolerances in Concrete Slabs using TLS data and the 2D Continuous Wavelet Transform

Nisha Puri[a], Enrique Valero[b], Yelda Turkan[a*], Frédéric Bosché[b]

[a] *School of Civil and Construction Engineering, Oregon State University, Corvallis, OR 97331, USA*

[b] *School of Energy, Geoscience, Infrastructure and Society, Heriot-Watt University, Edinburgh EH14 4AS, UK*

Abstract

While several concrete waviness assessment methods are being developed to overcome the disadvantages of one assessment method over the other, the sparseness of measurements associated with each method prevents from achieving a better understanding of how elevations and undulations change across the surface. Assessing waviness over multiple one-dimensional (1D)-survey lines may not accurately reflect the actual condition or waviness of the entire floor. The methodology presented in this paper presents a compliance-checking algorithm for detecting elements where dimensions exceed specified tolerance. It also enables assessment of a concrete surface in two-dimensional (2D) domain using the synergy of Terrestrial Laser Scanning (TLS) and Continuous Wavelet Transform (CWT). 2D CWT analysis provides information not only about the periods of the surface undulation, but also the location of such undulations. The validity of the methodology is established by running a test on point clouds obtained from a warehouse project near Gresham, Oregon. A rigorous comparison between one of the existing floor waviness measurement methods, the waviness index method, and the proposed method is made. The results showed that the proposed methodology delivers accurate results that enable the localization of surface undulations of various characteristic periods. Furthermore, the proposed method is more efficient in terms of time taken for acquiring the measurements, and is, thus, more cost efficient.

Keywords: Dimensional Quality Control, Tolerance Compliance, Terrestrial Laser Scanning, Point Cloud, Continuous Wavelet Transform, Depth Map

---

* Corresponding author. Tel: +1 541 737 2631; E-mail addresses: purin@oregonstate.edu (N. Puri); E.Valero@hw.ac.uk (E. Valero); yelda.turkan@oregonstate.edu (Y. Turkan); F.N.Bosche@hw.ac.uk (F. Bosche).

1 Introduction

As-built dimensions of cast-in-place concrete elements often differ from the dimensions originally specified in as-designed plans [1]. Dimensional Quality Control (QC) verifies that elements are constructed in compliance with the specified dimensional tolerances. For instance, when combining precast and cast-in-place elements, checking dimensional tolerance of all elements is necessary for ensuring acceptable performance of joints and interfacing materials [2]. In addition, failure to detect the imperfections in newly constructed surfaces during the earlier stages of construction causes delays in carrying out necessary repair works [3]. The repair, demolition, removal and replacement of defective concrete elements entail additional costs that could amount to as much as 12% of the project contract value [3-6]. Thus, upon the completion of concrete elements, it is crucial to carry out inspections in a timely manner. Furthermore, traditional inspection procedures related to dimensional QC are labor intensive and time consuming.

Focusing on concrete slabs, several factors influence the dimensional quality of cast-in-place concrete slabs, such as sweltering temperatures, placement and finishing techniques that are applied during construction. Proper regulation and control of these factors are essential for achieving specified levels of waviness and levelness. The defects resulting from the waviness of concrete slabs not only create aesthetic issues but also affect the efficiency of lift trucks and very narrow aisle (VNA) vehicles. Even if waviness present in slabs is not immediately noticeable, the waviness of the concrete slabs in industrial facilities, such as large warehouses, must be strictly examined since failing to detect waviness and deviations from the specified tolerances can greatly affect the operational activities that the floor is designed to handle [8]. Figure 1 illustrates how irregularities on the floor affect the stability of VNA trucks. Variations in elevation between the left and right wheels (*d*) of a VNA truck results in static lean (*s*) of VNA trucks. The static lean can potentially increase up to ten times due to the waviness present in concrete slabs [9].
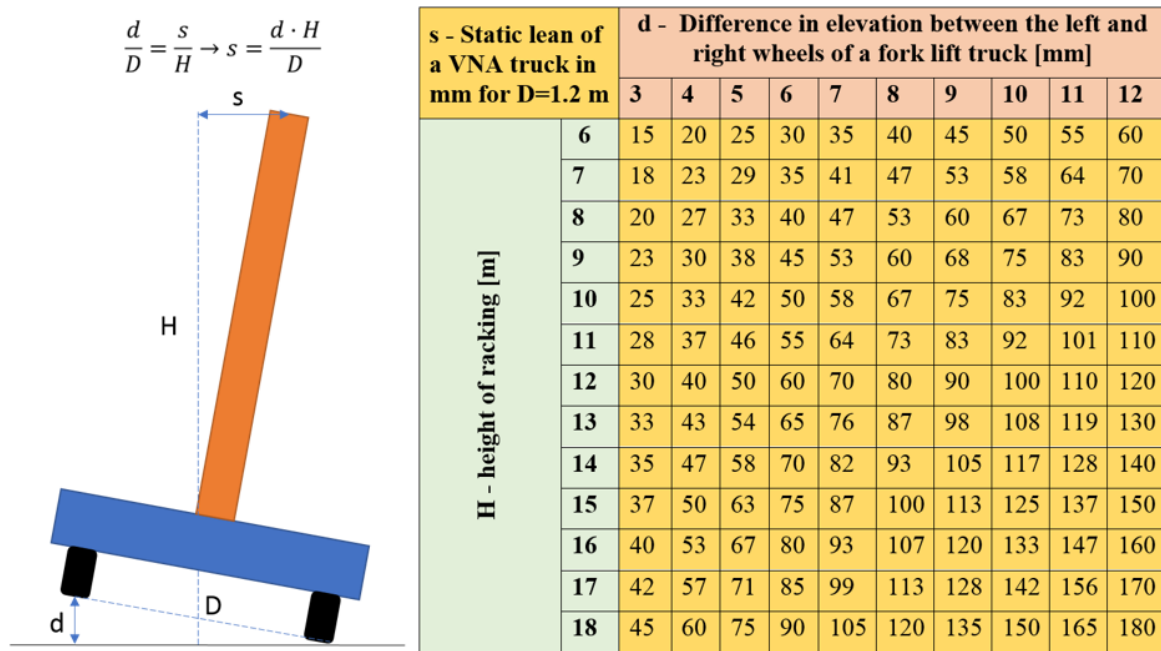
$$\frac{d}{D} = \frac{s}{H} \rightarrow s = \frac{d \cdot H}{D}$$

s - Static lean of a VNA truck in mm for D=1.2 m	d - Difference in elevation between the left and right wheels of a fork lift truck [mm]									
H - height of racking [m]	3	4	5	6	7	8	9	10	11	12
6	15	20	25	30	35	40	45	50	55	60
7	18	23	29	35	41	47	53	58	64	70
8	20	27	33	40	47	53	60	67	73	80
9	23	30	38	45	53	60	68	75	83	90
10	25	33	42	50	58	67	75	83	92	100
11	28	37	46	55	64	73	83	92	101	110
12	30	40	50	60	70	80	90	100	110	120
13	33	43	54	65	76	87	98	108	119	130
14	35	47	58	70	82	93	105	117	128	140
15	37	50	63	75	87	100	113	125	137	150
16	40	53	67	80	93	107	120	133	147	160
17	42	57	71	85	99	113	128	142	156	170
18	45	60	75	90	105	120	135	150	165	180

Figure 1 The effect of difference in elevation between the wheels on the static lean for a VNA

The methods for measuring concrete slab waviness, which are currently prevalent in the construction industry, require intensive human intervention, are tedious and time-consuming, and yet are based on sparse measurements. These methods entail the surveying of 1D lines for differences in elevations and characterizing undulations of specific periods.

The Straightedge method involves laying a 10-ft (3.05 m) Straightedge across a survey line on the floor and measuring the distance between the Straightedge and the floor using a stainless steel slip gauge [1]. While the results obtained with this method are easily comprehensible, the process of laying out the Straightedge over large surface areas is labor-intensive and engenders random errors in the measurements [10]. In addition, this time-intensive method provides information about the deviations between as-built and as-designed points only at relatively few measured points.

The introduction of the F-numbers method was aimed towards eradicating random errors in measurements, via the use of instruments that enable measurement of elevation differences at fix intervals to produce more accurate results. It provides the results in the form of two numbers: Floor Flatness (FF) and Floor Levelness (FL). FF describes the flatness associated with the measured floor surface point, whereas FL describes the levelness of the measured floor surface point. As

43 described in the ASTM E1155-14 standard [11], the measurements are carried out at intervals of

44 1-ft along each survey line, and the measurements collected from multiple survey lines are

45 statistically processed to generate FF and FL numbers that describe the conditions of the entire

46 floor surface. In addition, results produced from the F-number method are in the form of flatness

47 numbers (F_F and F_L values) that are hard to comprehend.

48   The Waviness Index (WI) method, as described in ASTM E1486-14 [12], was developed later

49 because the F-number method provides information only about the floor undulations with periods

50 of 1.5 to 4-ft (0.46 – 1.22 m) and 15 to 80-ft (4.6 – 24.4 m). In contrast, the WI method identifies

51 various periods of floor undulations between 2-ft and 10-ft, which correspond to the periods of

52 surface undulation that affect the operation of forklifts [13][8][14]. The results obtained using the

53 WI method are expressed in inches and are relatively easier to comprehend.

54   Despite having a significant advantage over the Straightedge and the F-number methods, the

55 WI method shares similar drawbacks with those methods. Sparse measurements yielded by the

56 three methods fail to guarantee that the collected data is an accurate representation of the geometric

57 features of the surface. Although results may be repeatable with a certain error, they fail to capture

58 the geometric details of the entire 2D floor surface and essentially do not impart information about

59 the waviness of the 2D surface. Data collection from large surface areas using these methods

60 demands significant amount of time and manual labor. Since these methods require measurement

61 tools to be manually moved across the surface of the floor, the results obtained are prone to human

62 error. Random errors, which potentially arise due to possible carelessness exerted while handling

63 the measurement instruments, contribute toward inaccuracies in measurements. Moreover, the

64 inability to retrieve similar results between different measurement sessions is one of the prominent

65 drawbacks of these methods. And finally, applying these methods to measure the floor waviness

66 of large floor areas, such as warehouse projects, is quite difficult. It is important to note that

67 warehouse projects typically have floor surface areas that are larger than 4,000 m^2. Consequently,

68 using these methods for such projects generate results that are not repeatable. In addition, the

69 obtained results are limited in the orientation of the defects and the range of wavelength.

70 Furthermore, the inability to explicitly reveal the location of those undulations remains a

71 disadvantage for these methods [8].

72   The F-number and WI methods reflect the state-of-the-art practices in measuring the waviness
73   of concrete slabs. To overcome the challenges arising with these methods, newer technologies,
74   such as terrestrial laser scanning (TLS), can be leveraged to measure surface waviness in a more
75   efficient manner. The ability of a TLS device to accurately capture the geometric information of
76   concrete surfaces provides an opportunity to reconsider the assessment of surface waviness using
77   traditional measurement instruments.

78   The objective of this study is to develop a methodology that uses TLS to obtain accurate
79   waviness information about newly constructed and existing concrete surfaces rapidly. This paper
80   presents a methodology that applies the two-dimensional Continuous Wavelet Transform (2D
81   CWT) to TLS point clouds to measure concrete slab surface waviness. The proposed methodology
82   is designed to help carry out tolerance compliance control tasks for slabs based on project
83   specifications describing their waviness tolerances. Uniquely, the methodology is able to perform
84   an accurate and comprehensive assessment of the surface geometry in both spatial and frequency
85   domains. The features pertaining to the proposed and existing methods are summarized in Table
86   1.

87   Table 1 Features and performance of existing standard methods and the proposed method for
88   measuring floor flatness.

	Method	Straightedge	F-Number	Waviness Index	2D CWT
Features	**Periods of undulation detected**	10'-20' (3.05 – 6.10 m)	1.5' – 4' (0.46 – 1.22 m) (F_F) 15' – 80' (4.57 – 24.38 m). (F_L)	2' – 10' (0.61 – 3.05 m)	Any
	Output	Values in Inches	F_F and F_L values	Values in Inches	Map showing detected undulations for various periods
	Types of errors	Random and systematic error	Random error	Random error	Systematic error (±3 to ±6 mm)

	Data acquisition efficiency (approx.) (sec/m²)	7	4	4	2
	Point Sampling	Along 1D non-parallel survey lines in 10-foot segments	Along 1D parallel survey lines in two orthogonal directions	Along 1D parallel survey lines in two orthogonal directions	Across 2D surface
	Sparsity of measurements	No	No	No	Yes
Performance Criteria Achievement	**Localization of defects**	No	No	No	Yes
	Visualization of region of defects	No	No	No	Yes
	Repeatability	No	No	No	Yes

89

90   The rest of the paper is structured as follows. Section 2 provides background information
91 on the utilization of TLS point clouds for project and QC, and the application of discrete and
92 continuous wavelet transforms for surface characterization. Section 3 then introduces the proposed
93 method for characterizing surface waviness of concrete slabs and discusses the various stages of
94 pre-processing and processing the TLS point cloud data. The proposed methodology is validated
95 using data obtained from a warehouse construction project. The experimental results are provided
96 and discussed in Section 4. The final section draws conclusions and discusses directions for future
97 research.

2   Research Background

2.1   Dimensional Tolerances for Floor Flatness and Waviness

The dimensions of newly constructed and existing building elements can vary, slightly or significantly, from the dimensions specified in the design documents [1]. Tolerances, or allowable deviations in those dimensions, are typically specified during the design phase for different measures such as length, width, thickness, perpendicularity, or verticality. Standard ACI 117-90, for example, provides a comprehensive list of tolerance criteria for cast-in-place concrete elements, such as vertical, lateral, and level alignments, and cross-sectional dimensions. The specified dimensional tolerances are an output of economical and practical considerations [15]. The role of QC inspectors is to ensure that the appropriate/specified tolerance values are achieved as construction progresses. Inaccuracies in the geometry of concrete elements during construction arise from improper establishment of a reference system for controlling the alignment, manual measurements, poor workmanship and in some cases, the method used for measurement [16].

2.2   TLS Point Clouds for Project Control

Acquisition of accurate project as-built data is crucial for dimensional quality control measurements, so that informed decisions can be made in a timely manner. TLS is a modern surveying technology that has been gaining increasing popularity in the Architectural, Engineering, Construction and Facilities Management (AEC&FM) industry. The versatility of the TLS technology has been tested in various fields of AEC&FM. For example, TLS has been used in remotely assessing the conditions of environments where human access is difficult or dangerous [17], for generating BIMs that represent the as-built conditions of building facilities [18], as well as construction progress control [15–19].

2.2.1   TLS Point Clouds for Quality Control

The use of TLS for dimensional QC is gaining interest due to its ability to rapidly provide inspectors with project as-built data in the form of both dense and accurate 3D point clouds (sub mm to mm-level accuracy) [24]. Using TLS not only solves the problems associated with accuracy and repeatability, but also enables the acquisition of data that represents the geometry of entire surfaces, thereby addressing the data sparsity limitations of existing surveying methods. Focusing

126   on flatness measurement, compared to existing measurement tools employed in current standard

127   flatness measurement methods, TLS thus offers an efficient way of collecting dense as-built data

128   covering entire slab surface.

129   Regarding the processing of TLS data for QC, Fuchs et al. [25] and Shafer and Weber [26]

130   developed deformation monitoring algorithms to find the differences in positions of TLS data

131   points with respect to a reference surface. In [27], a color map generated from the TLS data was

132   used to assess the flatness of facades in a multi-story building and the additional costs arising from

133   placing excess mortar on these facades was evaluated based on the volumetric quantities derived

134   from TLS data. In [28], a methodology that identifies the geometric irregularities in precast

135   concrete elements by comparing as-built data obtained from TLS and as-designed data obtained

136   from BIM was developed. Tang et al. [7] developed three algorithms which helped in finding the

137   difference in elevation of the points in the point cloud with respect to a plane taken from a BIM

138   model or a plane specified by the user. The method described in [29] used an elevation map where

139   each interval in height were represented with different colors. This approach represented the height

140   of each point with respect to a reference plane obtained from a BIM model. All the proposed

141   methodologies and existing approaches detected areas where different degrees of deviations

142   occurred, however they have failed to characterize the waviness or the periods of surface

143   undulations.

144   Using 3D point clouds obtained from TLS and as-designed geometry information from BIM,

145   Bosché and Guenet [30] developed an approach based on BIM and TLS data to assess whether the

146   geometry of as-is elements adhere to the specified surface flatness tolerances. An experiment was

147   conducted to compare the results obtained using the proposed method with the ones obtained from

148   Straightedge and F-number methods. The digital application of Straightedge and F-Number, as

149   presented in that study, significantly reduces the time required for data collection and analysis,

150   compared to traditional methods. However, flatness analysis remains conducted along sparsely

151   surveyed 1D survey lines, which delivers results limited in spatial and wavelength resolution.

152   Bosché and Biotteau [8] developed a method that applies 1D CWT to TLS data to characterize

153   surface undulation   periods. That approach addresses the limitation of previous works in

154   wavelength resolution, i.e. the approach examines surface waviness at a wider range of

155   wavelengths or characteristic periods. However, the study remains based on measurements along

156   1D lines that do not enable an analysis of flatness in all possible directions, and still provide results
157   with limited spatial resolution. Valero and Bosche [31] presented preliminary results on the
158   application of the 2D CWT to TLS data and compared the results with the WI method using
159   laboratory experiments. The work presented here expands on this and delivers a 2D analysis of
160   surface data in a more comprehensive manner using a larger and more representative concrete slab
161   as case study.

162   ## 2.3   Wavelet Transform for Surface Characterization

163   Wavelet Transform (WT) has a wide range of applications in engineering, some of which
164   include seismic signal analysis [32], sound pattern analysis [33] and quantum mechanics [34]. WT
165   is also widely used in the area of surface texture characterization, where it is used to break down
166   the 2D profiles of surfaces into the roughness and waviness components [35]. WT has been applied
167   to characterize surface roughness and waviness in several studies, and it has many applications in
168   the field of point cloud processing such as point cloud de-noising and rock surface roughness
169   quantification [31–33]. A technique using 1D WT for characterizing different types of surfaces
170   was introduced by Chen et al. [39]. Josso et al. [40] performed 2D multi-scaled decomposition
171   using images instead of profiles. Stępień and Makieła [41] applied 2D WT to analyze the
172   deviations of cylindrical surfaces. Jiang et al. [42], Coiffman and Maggioni [43] and Hussein et al.
173   [44] described the concepts of lifting wavelets and diffusion wavelets and used them for surface
174   filtering. WT can be extended from 1D analysis to multi-dimensional signals as well [8][45]. Some
175   applications of 2D CWT include characterizing the wavelengths of landslide areas and identifying
176   the regions having high risk of landslides using topographic images [46]. Additional information
177   about the different types of wavelets and the application of wavelet transform, can be found in [47]
178   and [48]. And, as reviewed above, the CWT has been previously suggested in [8] and [31] for use
179   in construction surface flatness assessment.

180   ## 2.4   Continuous Wavelet Transform

181   The continuous wavelet transform (CWT) of a given function is the inner product of the
182   function with the scaled and shifted versions of the mother wavelet [47]. The output of the inner
183   product is the wavelet coefficient at a specific time or location and scale [48]. In order for a

184   function, $\psi(t) \in L^2 (\mathbb{R})$, to qualify as a mother wavelet, it has to satisfy a condition known as the

185   admissibility condition as stated below [49]:

$$0 < C\psi := \int_{-\infty}^{\infty} \frac{|\psi(\omega)|}{|\omega|} d\omega < \infty \qquad (1)$$

187   where, C_ψ is the admissibility condition and ω is the angular (or radian) frequency. This

188   condition can also be written as [49]:

$$\Psi(0) = \int_{-\infty}^{\infty} \psi(t) dt = 0 \qquad (2)$$

190   This implies that the function $\psi(t)$ has to move above and below the t-axis in a wave-like

191   manner with decaying properties. Figure 2 demonstrates such properties with the example of a

192   typical wavelet function commonly known as the Mexican Hat wavelet.

193
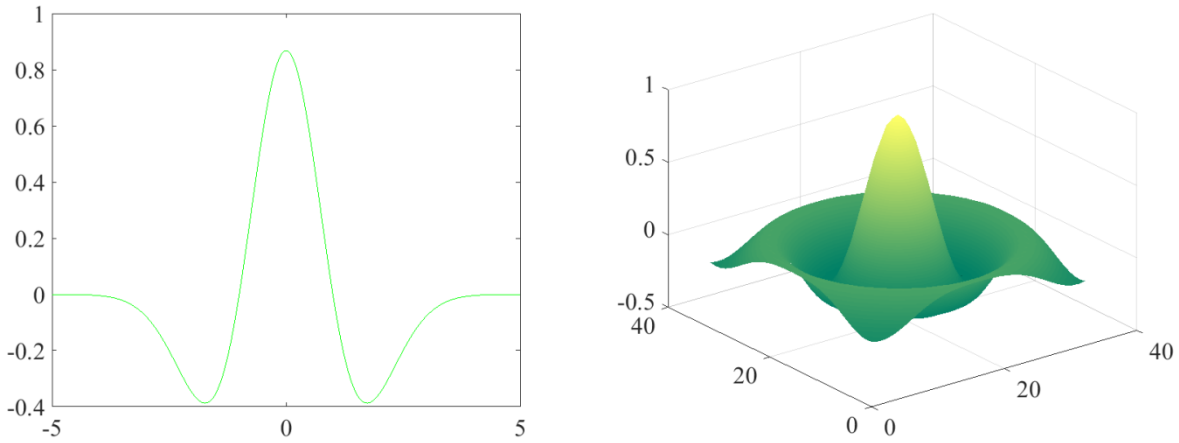
194   Figure 2 1D (left) and 2D (right) Mexican Hat Wavelet

195   CWT can be used to describe the time and frequency components of a temporal signal in

196   detail. 1D CWT involves taking the original function and displaying the output function in terms

197   of two variables, which are time and scale. The spectral information about a 2D signal for any

198   scale s and location (x, y) is given by the 2D CWT [50], that is an extension of the 1D CWT and

199   can be represented as follows [51]:

$$CWT (a, b, s) = \frac{1}{s} \int_{-\infty}^{\infty} \int_{-\infty}^{\infty} g(x,y) \psi_{abs}(x,y) \, dx dy \qquad (3)$$

201   where, $\psi_{abs}(x,y)$ is the mother wavelet, $g(x,y)$ is the continuous 2D signal, s is the scale

202   (dilating parameter) and (a,b) represents the location (translating parameter).

203   Different values of the translating and dilating parameters of the mother wavelet help in

204   describing the different frequencies of undulations present in the surface [52]. The convolution of

205   ψ and g provides the wavelengths (or periods) of the undulations present in the surface. The

206   coefficients *CWT (a, b, s)* quantify the degree of correlation between the wavelet ψ and the

207   function *g* at each point. In this way, apart from analyzing signals in time and frequency, the CWT

208   can be extended to analyze signals, together in space and scale (space-scale analysis).

209   Different wavelets can be used as the mother wavelet to detect different types of

210   undulations. The selection of an appropriate type of wavelet determines how efficiently the

211   different components of a signal are extracted [53]. The geometric shapes of the wavelet is

212   considered an important criteria when selecting the type of mother wavelet in [54]. The

213   resemblance between the shape of the wavelet and the geometric features of a signal provides a

214   cue for the selection of an appropriate wavelet. The defects present in as-built or as-is concrete

215   surfaces resembles waves in the form of small bumps and dips, and the shape of 2D Mexican Hat

216   wavelet closely resembles the shape of the surface undulations present on concrete surfaces, as

217   shown in Figure 2. The Mexican Hat wavelet is a real and isotropic wavelet that is good for

218   detecting contour features [55][56]. The use of different values of the translation and scale

219   parameters of the mother wavelet enable the detection of undulations corresponding to different

220   characteristic periods in the point cloud data. Therefore, it is chosen as the mother wavelet in this

221   study. 2D Mexican Hat wavelet in spatial domain is depicted as follows:

222        $$\psi(x,y) = \frac{1}{2\pi}(2 - x^2 - y^2) * e^{-\frac{1}{2}(x^2 + y^2)} \hspace{3cm} (4)$$

223

2.5   Contribution

224

225   Floor flatness testing is typically performed to assess how well the contractor has performed

226   the work based on the specifications. Failure to carry out floor flatness measurements within a

227   specific time window may yield inaccurate results and does not accurately reflect the contractor's

228   performance. This can be attributed to the increase in curling of the joints and cracks in the concrete

229   slabs with the age of concrete. Therefore, the American Concrete Institute (ACI 117-10) [57]

230   requires that floor flatness testing on any concrete slab should be performed within 24 hours for

231   best results, and no later than 72 hours, after the concrete placement, unless clearly stated otherwise

232   in the specifications.

233   The major contribution of this paper is to present a new approach for floor flatness control

234   using the 2D CWT applied to TLS data. The approach builds on preliminary works published in

235   [33], but presents and analyses it in a more comprehensive manner. In particular, a warehouse

236   concrete slab having been scanned within 10 hours of having been poured is used as a

237   representative real-life case study. The overall time required for scanning the worksite is less than

238   the time associated with data collection using the traditional methods of waviness measurement.

239   The waviness results obtained using the proposed approach are validated by establishing a

240   correlation between results obtained using the proposed approach and the WI method. The

241   correlation shows that the proposed method generates results that supersede those that are obtained

242   using the WI method.

243   3   Proposed Methodology

244   The proposed methodology, as summarized in Figure 3, follows the approaches developed in

245   [31] in order to characterize surface waviness. The raw 3D point cloud consists of data points from

246   a concrete slab as well as its surrounding environment, including workers, equipment and

247   surrounding buildings. The point cloud is typically the result of multiple laser scans co-registered

248   using a standard (reliable) target-based approach. First, the raw point cloud is pre-processed to

249   isolate the area of interest, the concrete slab in this case, from the raw point cloud. The next step

250   is to develop a depth map, which is used as input to the 2D CWT. The areas with undulations

251   corresponding to various characteristic periods are identified after applying the 2D CWT with the

252   Mexican Hat wavelet.

253

Raw Point Cloud Data → Remove noise from the unified point cloud → Convert Point Cloud to 2D depth map → Apply 2D CWT to Depth Map

Assess compliance with specifications ← Surface Waviness Characterization Results ← Detect and Localize Undulations

254
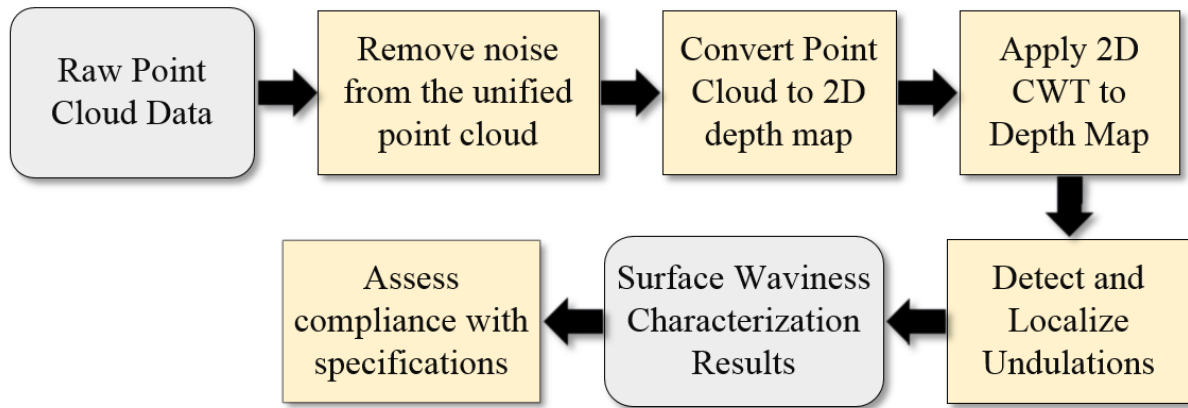
Figure 3 Overview of the research methodology

3.1 Data pre-processing

As stated in the overview of the research methodology, the raw point cloud data should be pre-processed before 2D CWT can be applied to it. The input is a raw point cloud that may be the result of the co-registration of multiple scans collected during the scanning process. The noise present in the registered point cloud data is removed using a corresponding functionality provided by a commercial point cloud processing software, leaving a clean point cloud of the area of interest (i.e. concrete slab). The pre-processed point cloud corresponding to the slab surface is aligned (parallel) to the xy plane, which is likely to be the case already. Accordingly, z coordinates represent the elevation of each point, facilitating further analysis.

In order to analyze the frequencies of undulations present on the surface, the point cloud data should have equispaced rows and columns along the x and y axes [58]. Because raw point cloud data from slabs typically has a random arrangement, it is converted into a regular grid, with intervals along the x and y axes were both set to $\delta_p = 1$ cm. This sampling interval ensures robust localization of defects across the 2D surface. Triangulation-based linear interpolation is used to obtain the values of z-coordinates at each grid point. Consequently, a 2D depth map is created, which represents the height of the surface for points at $\delta_p = 1$ cm intervals along the x- and y-axes.

3.2 Detection of Undulations using 2D Continuous Wavelet Transform

The depth map resulting from the previous operation is used as the input "signal" to the 2D CWT. The scale a at which the CWT is applied relates to a few parameters, as in Equation 5 [48]:

$$a = \frac{f_c}{f . \delta_p} = \frac{T . f_c}{\delta_p} \qquad (5)$$

where f represents the frequency of the undulation, T the characteristic period of the signal, and f_c, the main frequency component of the Fourier Transform of the mother wavelet. For the Mexican Hat wavelet, $f_c = 0.252$ cm^{-1}.

The output of applying the 2D CWT is a series of scalograms that report the CWT response at each grid point on the depth map. These maps are meaningful to some extent, but should be further processed to accurately define the exact characteristic period at each location. Indeed, a wavy region will result in peak responses at several scales, i.e. frequencies, as can be seen in Figure 77 for example. However, not all those peaks correspond to defects whose size matches the period associated to that scale. For this, we follow the strategy initially suggested in Valero and Bosché in [31]. First, peak values (i.e. local maxima) are detected in each 2D CWT response map. Next, different isolines are then calculated around each peak, which connect pixels with the same CWT response. These isolines may describe irregular shapes whose mathematical analysis, and further comparison with other defects, can be truly complex. Therefore, areas enclosed by isolines are described by means of ellipses, and the two main axes of each ellipse are determined to be used as reference values. If any of the axes matches the period associated to the scale of interest, a surface deviation is detected in that area for that particular period.

The result of this process is a set of clear waviness defect detections at all the scales/periods considered, which can be combined in a single diagram.

3.3 Correspondence between WI and 2D CWT methods.

The correspondence between the WI method and the 2D CWT method in terms of their response to similar surface wavelengths (or periods) is shown in Table 2. The k values of the WI method correspond to characteristic periods of different lengths. The corresponding CWT scales for each of these k values are calculated using equation 5 with $\delta_p = 1$ cm. The characteristic

299 periods *(T)* selected in this table represent the floor undulations, with periods of 2, 4, 6, 8 and 10

300 ft, that are the focus of the WI method.

301 Table 2 Continuous Wavelet Transform scales and equivalent Waviness Index [8]

Characteristic period (T) [cm]	CWT scale (a)	Waviness Index (k values)
61	15	1
121.9	30	2
182.9	45	3
243.8	60	4
304.8	75	5

4 Experimental Results

4.1 Data Collection and Pre-Processing

304 An in-situ concrete slab from a warehouse project in Gresham, Oregon was scanned after

305 5-6 hours of placement. The surface of the concrete slab was sturdy enough for foot traffic and for

306 setting up the tripod of the scanner. The concrete slab of the warehouse building was scanned using

307 a Leica ScanStation P40 3D laser scanner. The scanner has 8" horizontal and 8" vertical angular

308 accuracy. The 3D position accuracy is ±3mm at 50 m and ±6 mm at 100 m [59].

309 Figure 4 shows the plan view of the concrete slab as well as one of the 3D point clouds captured.

310 The area of interest with a surface area of approximately 1500 m^2 is highlighted in both the plan

311 view and the point cloud. It was determined that scans taken from four different locations would

312 be sufficient to capture the surface with sufficient detail. Six targets were placed at different

313 locations on site to facilitate the point cloud registration process.
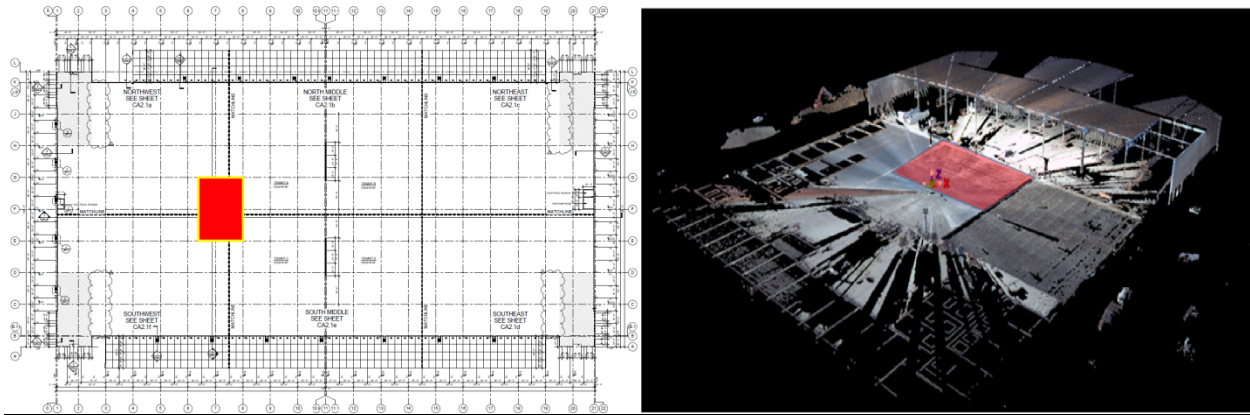
Figure 4 The floor plan (left) and the 3D point cloud (right) of the warehouse building. The area of interest is highlighted in red.

The overall scanning process, including setup, scanning, dismantling and re-locating, took approximately 45 minutes. The data pre-processing stage, comprising of registering the point clouds in the same coordinate system and removing the noise, took 50 minutes. The raw point clouds, i.e. laser scans including noise, were first imported into a commercial point cloud processing software. The four laser scans were registered under the same coordinate system using the targets placed at strategic locations on the construction site. After the registration was complete, the point cloud of the area of interest was manually isolated from the rest. The point cloud corresponding to the slab section of interest had approximately 100,000,000 points. Figure 5 shows an image of the scan after registration and noise removal.

326
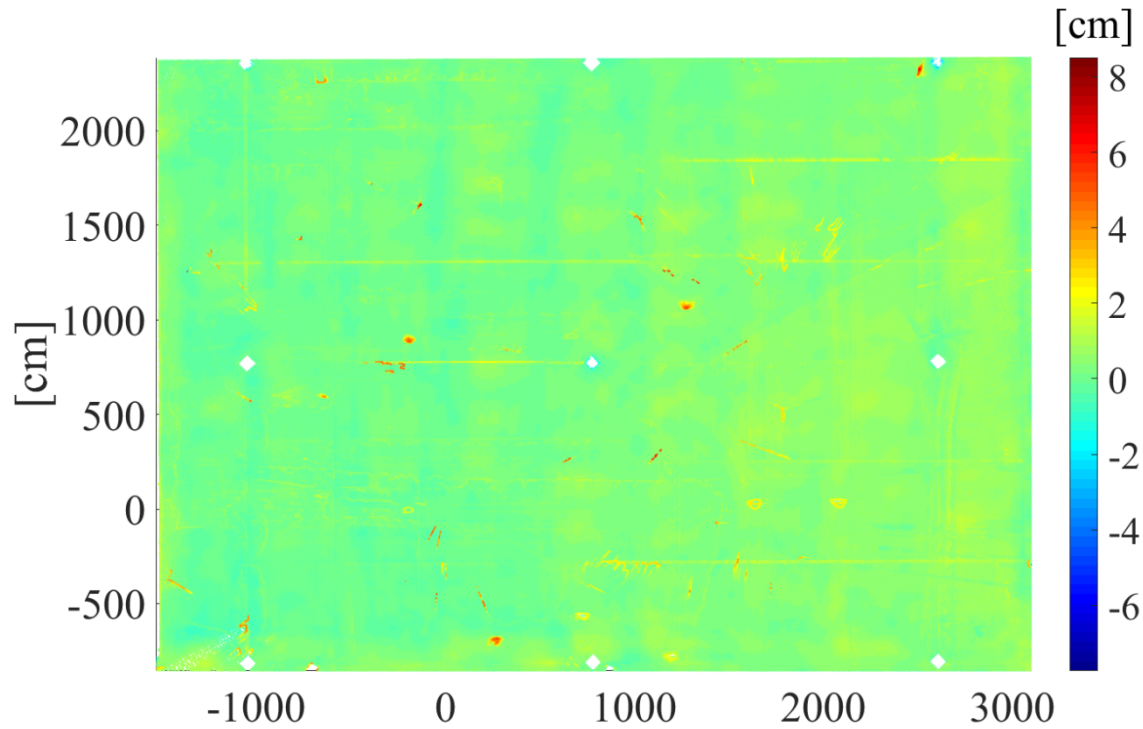
Figure 5 Top view of the point cloud of the area of interest obtained after the registration of the four scans and noise removal. The color scale represents elevation values in cm.

4.2 Data Processing

Following pre-processing, the point cloud is converted into a 3242 x 4629 depth map with 1 cm intervals in both horizontal and vertical directions, with the z-coordinates at each grid point calculated as described in Section 3.1. Figure 6 shows the resulting depth map. As seen in Figure 6, the height of the concrete slab with respect to the xy plane, varies most in the interval of -2 cm to 2 cm. Thus, the color map was adjusted accordingly to highlight the height differences between various areas across the floor.
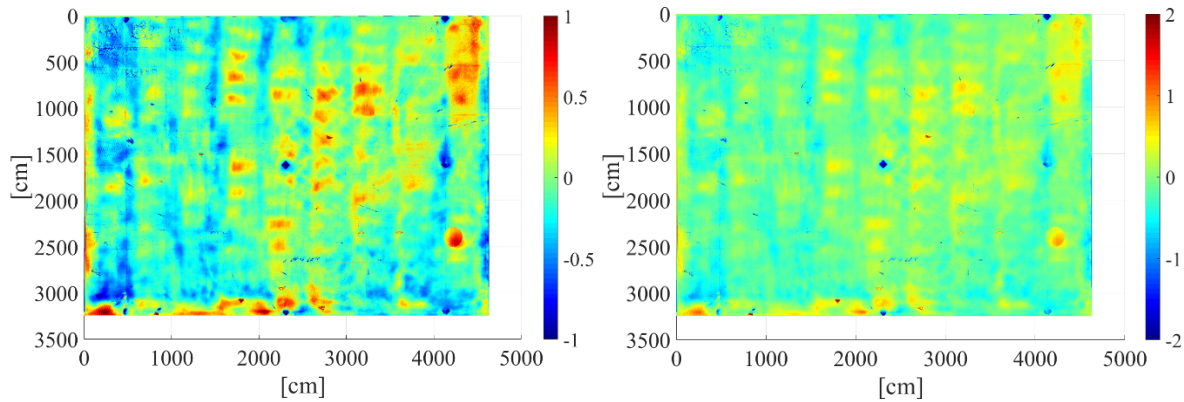
Figure 6 Depth map derived from the TLS data, with color map limits set to [-1, 1] cm (left) and [-2, 2] cm (right)

4.3 CWT Results

4.3.1 CWT Scalogram

Figure 7 presents the results obtained using the scales (*a*) 15, 30, 45, 60 and 75 of the mother wavelet. The regions where the input "signal" strongly correlates with the mother wavelet applied at the scales above are highlighted in yellow in Figure 7.

The point cloud in Figure 5 and the depth maps in Figure 6 show that the surface of the investigated slab is relatively flat with a few "peaks". For the entire slab surface, the average value of the deviation in the z-axis was 0.0 cm with a standard deviation of 0.3 cm. Figure 7(a) represents the regions where the wavelength of the undulations present on the surface correlates with the mother wavelet of scale 15. The scalogram shows that the regions near (1900 cm, 3100 cm) has an undulation of this characteristic period present on the slab surface. Figure 7 (b) shows regions near (1900 cm, 3100 cm) and (2400 cm, 1700 cm) have undulations that correspond to the mother wavelet of scale 30. Similarly, the scalograms in Figure 7 (c), (d) and (e) show that the region near (2400 cm, 1700 cm), (300 cm, 3400 cm) and (4200 cm, 2400 cm) have undulations corresponding to scales 45, 60 and 75. The region near (2400 cm, 1700 cm) shows responses for all these three scales. Thus, the identification of the scale which has the top response at that location is necessary. Furthermore, such analysis is an added advantage of using the proposed 2D CWT method and cannot be done using the WI method.
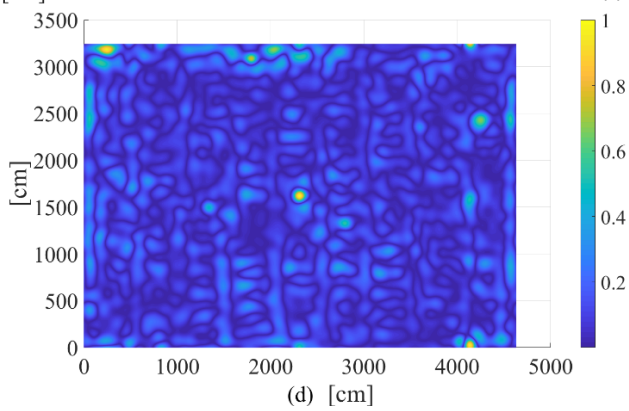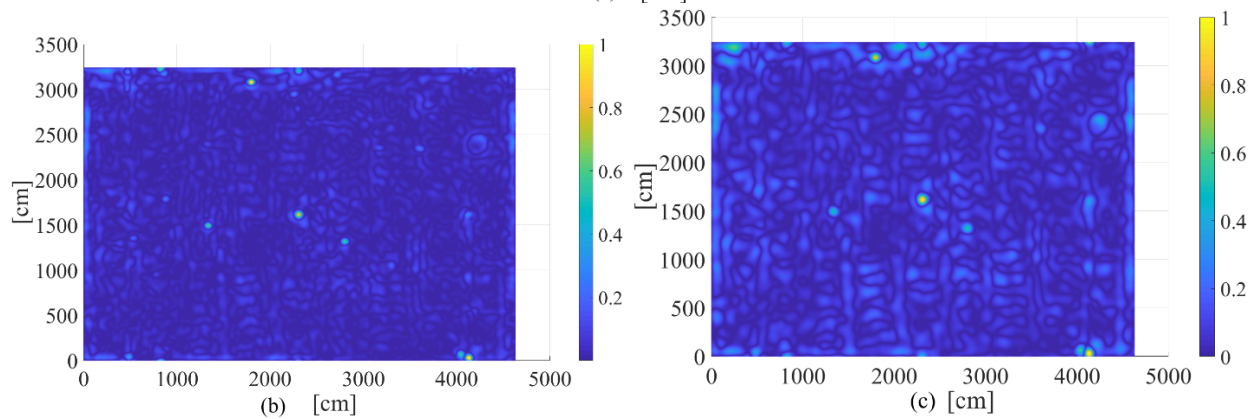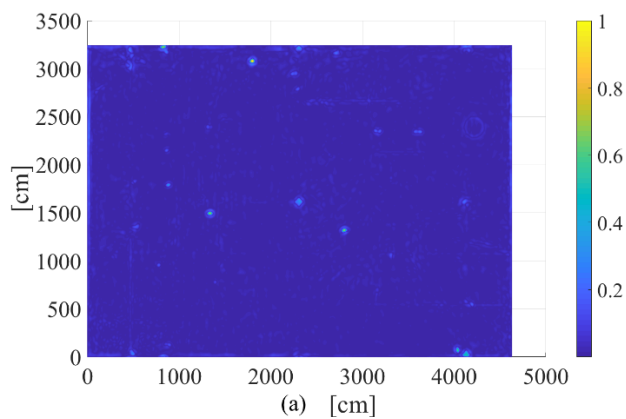
(a)

357

(b)

(c)

358

(d)

359

(e)

360
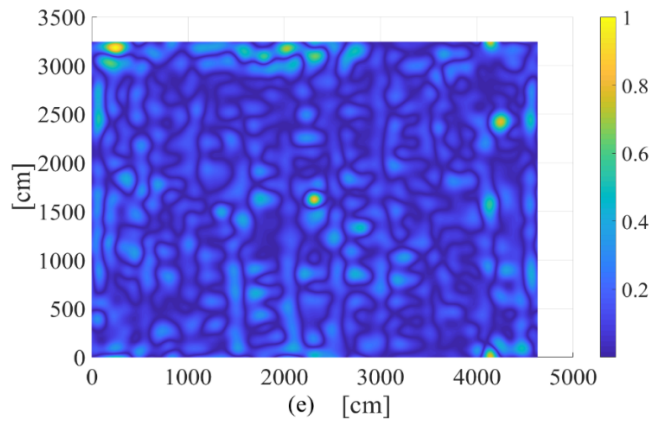
361   Figure 7 The coefficients obtained from the wavelet transformation corresponding to scales 15

362   (a), 30 (b), 45 (c), 60 (d) and 75 (e) are plotted on the map. The areas in the slabs where

363   undulations corresponding to these scales are present are shown.

4.3.2 Surface analysis and automatic defect detection

365   Figure 8 illustrates regions, enclosed by ellipses, where potential defects have been

366   identified for two of the five scales in Figure 7. Note that no defective regions were found for the

367   other three scales.

(a)   (b)
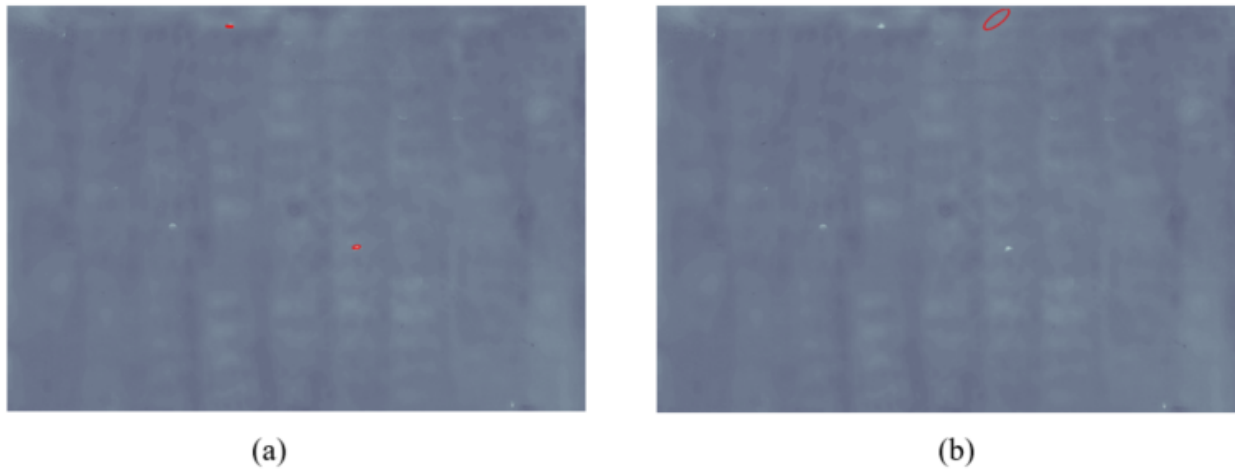
369   Figure 8 Potential defective areas for a) 61cm (±2cm) and b) 244cm (±2cm).

370   The advantage of our approach is that it combines dense 3D data from TLS with the 2D CWT that

371   can support the analysis of waviness with essentially any characteristic period (i.e. wavelength).

372   This enables our approach to study waviness not just for a few discrete wavelengths (like the 5

373   above), but for dense and large ranges of wavelengths. This is demonstrated in Figure 9 that

374   summarizes the potential defects on the slab for any wavelength within the continuous range of 20
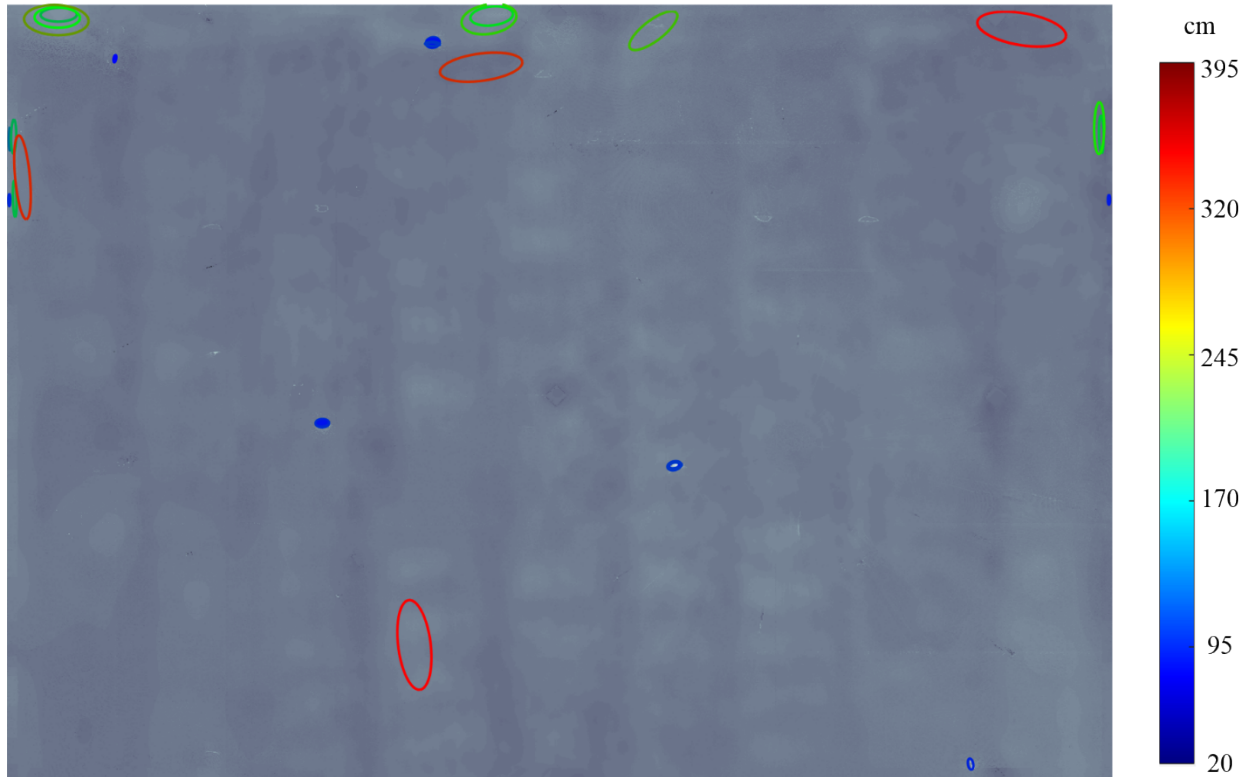
375   to 400 cm.

Figure 9 Detected defects for periods between 20 and 400 cm.

4.4   Comparison of Results with WI method

The ASTM E1486-14 standard describes the test method for measuring the waviness of concrete floors using the WI method. In a similar way to [8], we propose to apply the WI method as defined in this standard, but using the digitized slab surface as the surface of application (instead of the real slab). Referring to this standard, 103 survey lines along the x-axis and 148 lines along the y-axis were defined on the slab, as shown in Figure 10. The lines are spaced at 1-ft intervals. This is much denser that what would normally be achieved in normal practice, but is useful to conduct the comparison with the proposed CWT approach.
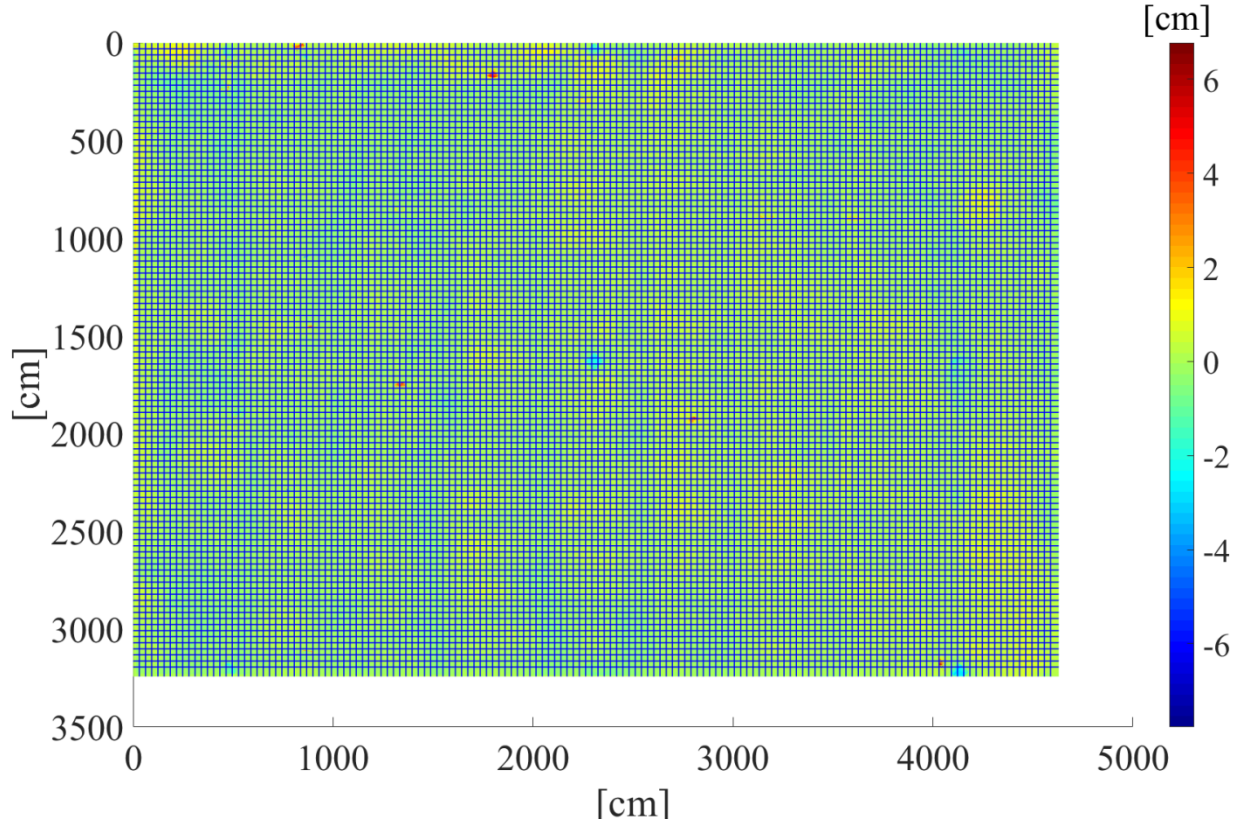
387 Figure 10 The 251 survey lines (103 along the x-axis and 148 along the y-axis) that are defined
388 across the slab surface.

389 The length adjusted RMS deviation *(LAD)* responses are calculated for each line. The survey lines

390 are parallel to each other and are spaced at a distance of 30.5 cm (1ft). Survey points with a spacing

391 *s*=30.5 cm (1ft) are measured along those lines. The standard defines chord length as the length of

392 the imaginary line joining two points on the surface of the concrete floor. The chord length is equal

393 to *2ks*, where k= {1, 2, 3, 4 and 5}. The vertical distance between the midpoint of the chord and

394 the survey point on the surface, D_{kj}, is calculated using the following formula,

395 $$D_{kj} = h_{j+k} - 0.5(h_j + h_{j+2k}) \qquad\qquad (6)$$

396 where, h_{j+k}, h_j and h_{j+2k} represent the heights of the survey point and the two end points of the

397 chord, respectively. These heights are obtained from the depth map calculated in section 4.2.

398 After the deviation D_{kj} is calculated, the length adjusted RMS deviation *(LAD_k)* is calculated using

399 equation 7.

$$400 \quad LAD_{l,k} = \sqrt{\frac{\frac{L_r}{2ks}[\sum_{i=1}^{jmax_{l,k}}(D_{l,k,j})^2]}{jmax_{l,k}}} \qquad (7)$$

401 where L_r corresponds to the reference length of 1 ft. $jmax_k$ corresponds to the total number of
402 deviation calculations with a chord length *2ks* along a survey line and l denotes the survey line
403 being tested.

404 Similarly, the 2D CWT responses at the jth sampled location, $CWT_{1,a,j}$, for scales 15, 30, 45, 60 and
405 75 were obtained in section 4.3.1. These scales correspond to the WI k-values 1, 2, 3, 4 and 5
406 respectively. It is proposed that the CWT responses for each of the 210 lines for those 5 scales,
407 $CWT_{l,a}$, be calculated using the similar formula:

$$408 \quad CWT_{l,a} = \sqrt{\frac{\sum_{i=1}^{jmax_{l,a}}CWT^2_{l,a,j}}{jmax_{l,a}}} \qquad (8)$$

409 where $jmax_k$ corresponds to number of locations at which the 2D CWT response have been
410 calculated.

411 The correlation between the $LAD_{l,k}$ and $CWT_{l,a}$ responses is calculated to compare the surface
412 waviness results obtained using the WI and 2D CWT methods. 15 survey lines along the x-axis
413 and 15 survey lines along the y-axis, as shown in Figure 11, are randomly selected (out of the
414 previously defined 251 lines), to illustrate the correlation results presented in Figure 12 and Figure
415 13. The correlation coefficients, denoted by r^2, are included in the top left-hand corner of each
416 graph. The values indicate a strong correlation between the results obtained using the WI and 2D
417 CWT methods. This strongly validates the value of the proposed approach, which has the
418 additional advantage of being able to more precisely define defects' wavelengths and locations
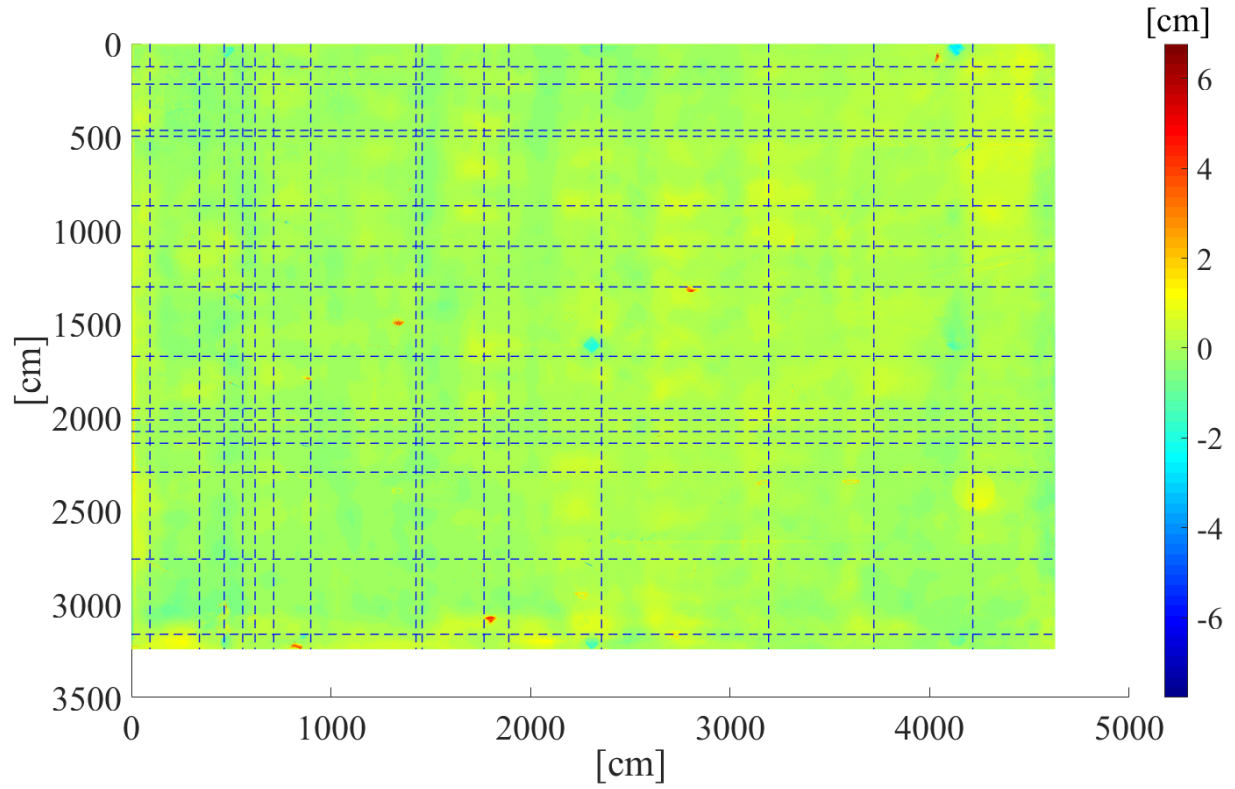419 (including actual orientation).

420

421 Figure 11 The 30 survey lines (15 along each axis) that were selected for the generation of
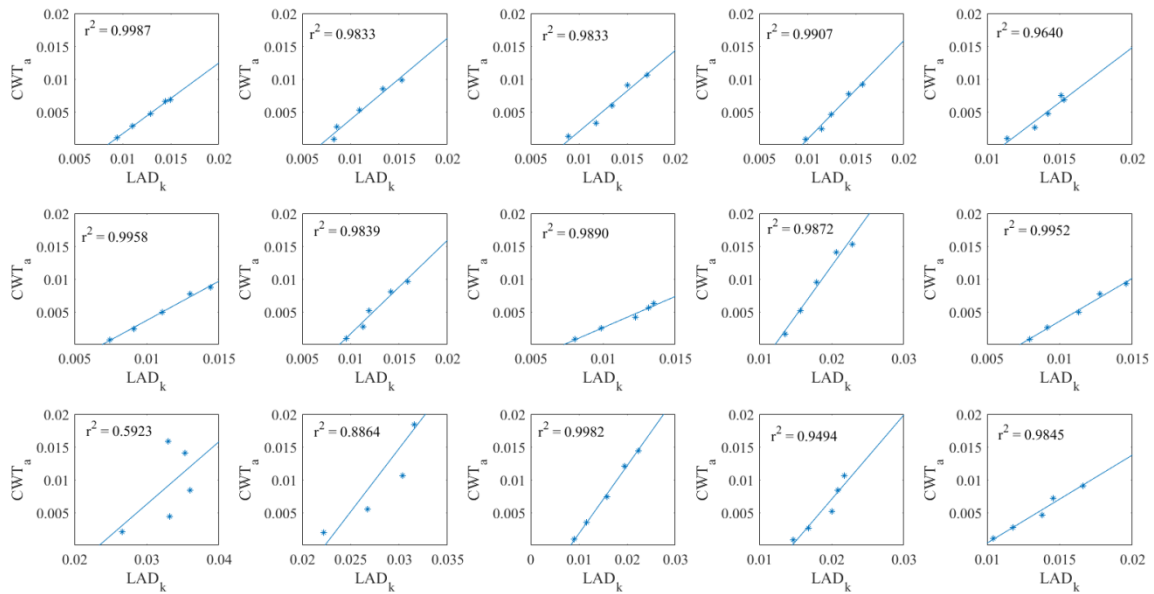422 correlation results.

423

424 Figure 12 Correlation between LAD$_{l,k}$ and CWT$_{l,a}$ responses for the five characteristic undulation
425   periods [61, 121.9, 182.9, 243.8, 304.8] cm, along 16 lines along the x-axis shown in Figure 11.
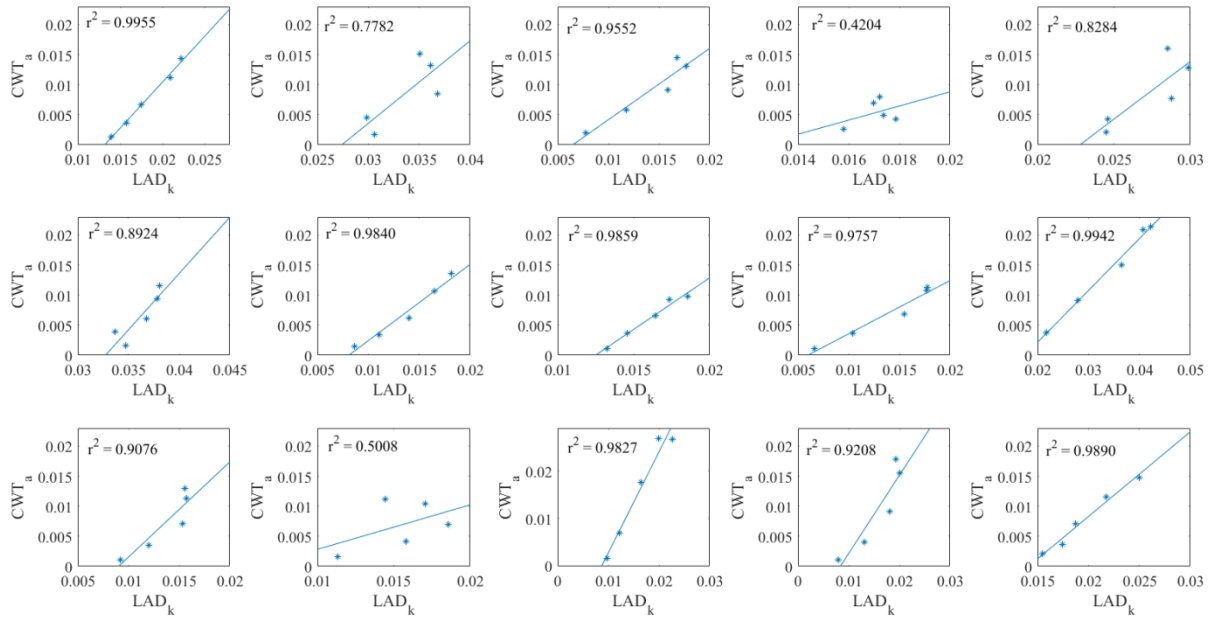

426

427 Figure 13 Correlation between LAD$_{l,k}$ and CWT$_{l,a}$ responses for the five characteristic undulation
428   periods [61, 121.9, 182.9, 243.8, 304.8] cm, along 16 lines along the y-axis shown in Figure 11.

429

430 The proposed approach overcomes all of the drawbacks of traditional waviness assessment
431 methods mentioned earlier. The 2D CWT method enables a comprehensive analysis of the
432 waviness of 2D surfaces, both in the spatial and wavelength domains. In contrast to the F-number
433 and WI methods, the output of the CWT-based approach enables easy visual representations of
434 where waviness defects are located on the surface (as shown in Figure 7). This can help users with
435 minimal knowledge about 3D TLS or 2D CWT to quickly determine where surface corrections
436 should be applied, for example.

5   Conclusions

438   TLS technology has a promising future in the construction industry owing to its ability to
439 rapidly and accurately capture and record as-built conditions. Research efforts are being
440 concentrated to identify specific areas, which could particularly benefit from the application of
441 TLS. Dimensional QC is one such area. The analysis performed using the 2D CWT for QC
442 provides great flexibility for examining the surface undulations with a wide range of characteristic

443 periods. The localization property of 2D CWT highlights regions on the surface and helps in
444 compliance assessment and corrective work planning.

445 The proposed approach in this paper demonstrates how TLS data of a concrete surface can be used
446 to characterize waviness by implementing 2D CWT, using Mexican Hat Wavelet as the mother
447 wavelet. The comparative analysis of the various methods of measuring waviness in concrete slabs
448 reveals that the 2D CWT method provides results that strongly correlate with those of the WI
449 method (the current state of the art), but has numerous advantages over it and other existing
450 methods.

451 Future research efforts can be directed toward improving the practicality of implementing laser
452 scanning for measuring floor surface waviness. The method proposed in this paper can be used in
453 conjunction with augmented reality devices to enable the visualization of undulations
454 corresponding to various characteristic periods on site. The proposed method can be further
455 improved by developing algorithms for automatically removing noise and generating scan plans
456 to estimate optimal scanning positions. For this study, manual effort was required for preparing
457 scan plans, setting up the scanner and collecting the point cloud data. A LiDAR integrated
458 Unmanned Aerial Vehicle (UAV) can also be used to collect the scans and automated registration
459 of laser scans can be further explored. Finally, a comparative analysis on using TLS and LiDAR
460 equipped UAVs for surface quality assessment can be conducted.

References

466 [1] D.K. Ballast, Handbook of construction tolerances, John Wiley, Hoboken, 2007, ISBN:
467 978-0-471-93151-5

468 [2] Manual for quality control for plants and production of structural precast concrete products,
469 Precast/Prestressed Concrete Institute, Chicago, IL, 1999,
470 http://www.enconunited.com/wp-content/uploads/2017/07/pci_mnl-116-
471 99_structural_qc_manual.pdf

472 [3] H.P. Gillette, C.S. Hill, C.T. Murray, H.B. Kirkland, S.C. Hadden, Engineering and
473   Contracting, The Myron C. Clark Publishing Company, 1913.

474 [4] J. L. Burati, J. J. Farrington, Costs of quality deviations in design and construction. Bureau
475   of Engineering Research, University of Texas at Austin, 1987.

476 [5] L. Patterson, W.B. Ledbetter, The Cost of Quality: A Management Tool, Excellence in the
477   Construction Project, American Society of Civil Engineers, 1989, pp. 100-105.

478 [6] P.-E. Josephson, Y. Hammarlund, The causes and costs of defects in construction,
479   Automation in Construction. 8 (1999) 681–687, https://doi.org/10.1016/s0926-
480   5805(98)00114-9

481 [7] P. Tang, B. Akinci, D. Huber, Characterization of three algorithms for detecting surface
482   flatness defects from dense point clouds, Three-Dimensional Imaging Metrology. (2009),
483   https://doi.org/10.1117/12.805727.

484 [8] F. Bosché, B. Biotteau, Terrestrial laser scanning and continuous wavelet transform for
485   controlling surface flatness in construction – A first investigation, Advanced Engineering
486   Informatics. 29 (2015) 591–601, https://doi.org/10.1016/j.aei.2015.05.002.

487 [9] F.R. Neal, Concrete industrial ground floors, Thomas Telford, London, 2002.

488 [10] B.M. Phares, G.A. Washer, D.D. Rolander, B.A. Graybeal, M. Moore, Routine Highway
489   Bridge Inspection Condition Documentation Accuracy and Reliability, Journal of Bridge
490   Engineering. 9 (2004) 403–413, https://doi.org/10.1061/(asce)1084-0702(2004)9:4(403).

491 [11] ASTM E1155-14 Standard Test Method for Determining FF Floor Flatness and FL Floor
492   Levelness Numbers, ASTM International, West Conshohocken, PA, 2014,
493   https://doi.org/10.1520/E1155-14

494 [12] ASTM E1486-14 Standard Test Method for Determining Floor Tolerances Using Waviness,
495   Wheel Path and Levelness Criteria, ASTM International, West Conshohocken, PA, 2014,
496   https://doi.org/10.1520/E1486

497 [13] C. N. Ytterberg, Using the Waviness Index To Improve Floor Flatness (1996).
498   http://www.concreteconstruction.net/_view-object?id=00000153-8bb9-dbf3-a177-
499   9fb958f40000

500 [14] R. E. Loov, Is the F-number system valid for your floor?, Concrete International. 12 (1990)
501   68–76.
502   https://www.concrete.org/publications/internationalconcreteabstractsportal/m/details/id/32
503   52

504 [15] DIN 18202 Tolerances in building construction – Buildings, Deutsches Institut für Normung
505   e. V., 2005.

506 [16] Latta, J. K., Inaccuracies in construction, Cracks, movements and joints in buildings,
507   National research council of Canada. (1976) 171.

508   [17]   G.S. Cheok, W.C. Stone, R.R. Lipman, C. Witzgall, Ladars for construction assessment and
509   update, Automation in Construction. 9 (2000) 463–477, https://doi.org/10.1016/s0926-
510   5805(00)00058-3.

511   [18]   H. Son, C. Kim, Semantic as-built 3D modeling of structural elements of buildings based
512   on local concavity and convexity, Advanced Engineering Informatics. 34 (2017) 114–124,
513   https://doi.org/10.1016/j.aei.2017.10.001.

514   [19]   S. Tuttas, A. Braun, A. Borrmann, U. Stilla, Comparision of photogrammetric point clouds
515   with BIM building elements for construction progress monitoring, ISPRS - International
516   Archives of the Photogrammetry, Remote Sensing and Spatial Information Sciences. XL-3
517   (2014) 341–345, https://doi.org/10.5194/isprsarchives-xl-3-341-2014.

518   [20]   A. Braun, S. Tuttas, A. Borrmann, U. Stilla, A concept for automated construction progress
519   monitoring using BIM-based geometric constraints and photogrammetric point clouds,
520   Journal of Information Technology in Construction (ITcon) 20 (5) (2015) 68-79,
521   http://www.itcon.org/2015/5

522   [21]   A. Braun, S. Tuttas, A. Borrmann, U. Stilla, Automated Progress Monitoring Based on
523   Photogrammetric Point Clouds and Precedence Relationship Graphs, Proceedings of the
524   32nd International Symposium on Automation and Robotics in Construction and Mining
525   (ISARC 2015). (2015), https://doi.org/10.22260/isarc2015/0034.

526   [22]   C. Kim, H. Son, C. Kim, Automated construction progress measurement using a 4D
527   building information model and 3D data, Automation in Construction. 31 (2013) 75–82,
528   https://doi.org/10.1016/j.autcon.2012.11.041.

529   [23]   H. Son, C. Kim, Y.K. Cho, Automated Schedule Updates Using As-Built Data and a 4D
530   Building Information Model, Journal of Management in Engineering. 33 (2017) 04017012,
531   https://doi.org/10.1061/(asce)me.1943-5479.0000528.

532   [24]   M.-C. Amann, T. Bosch, M. Lescure, R. Myllyla, M. Rioux, "Laser ranging: a critical
533   review of unusual techniques for distance measurement, Optical Engineering. 40 (1) (2001)
534   10-20, https://doi.org/10.1117/1.1330700

535   [25]   P. A. Fuchs, G. A. Washer, S. B. Chase, M. Moore, Applications of Laser-Based
536   Instrumentation for Highway Bridges, Journal of Bridge Engineering 9 (6) (2004) 541-549,
537   https://doi.org/10.1061/(ASCE)1084-0702(2004)9:6(541)

538   [26]   T. Schafer, T. Weber, Deformation measurement using terrestrial laser scanning at the
539   hydropower station of Gabcikovo, INGEO 2004 and FIG Regional Central and Eastern
540   European Conference on Engineering Surveying, FIG, Copenhagen, Denmark., 2004.

541   [27]   M.C. Israel, R.G. Pileggi, Use of 3D laser scanning for flatness and volumetric analysis of
542   mortar in facades, Revista IBRACON De Estruturas e Materiais. 9 (2016) 91–122,
543   https://doi.org/10.1590/s1983-41952016000100007.

544   [28]   Q. Wang, M.K. Kim, J.C. Cheng, H. Sohn, Automated quality assessment of precast
545   concrete elements with geometry irregularities using terrestrial laser scanning, Automation
546   in Construction. 68 (2016) 170–182, https://doi.org/10.1016/j.autcon.2016.03.014.

547   [29]   N.J. Shih, P.H. Wang, Using point cloud to inspect the construction quality of wall finish,
548   Proceedings of the 22nd eCAADe Conference, 2004, pp. 573-578,
549   http://papers.cumincad.org/data/works/att/2004_573.content.pdf

550   [30]   F. Bosché, E. Guenet, Automating surface flatness control using terrestrial laser scanning
551   and building information models, Automation in Construction. 44 (2014) 212–226.
552   https://doi.org/10.1016/j.autcon.2014.03.028.

553   [31]   E. Valero, F. Bosché, Automatic Surface Flatness Control using Terrestrial Laser Scanning
554   Data and the 2D Continuous Wavelet Transform, Proceedings of the 33rd International
555   Symposium on Automation and Robotics in Construction (ISARC). (2016),
556   https://doi.org/10.22260/isarc2016/0007.

557   [32]   P. Goupillaud, A. Grossmann, J. Morlet, Cycle-octave and related transforms in seismic
558   signal analysis, Geoexploration. 23 (1984) 85–102, https://doi.org/10.1016/0016-
559   7142(84)90025-5.

560   [33]   R. Kronland-Martinet, J. Morlet, A. Grossmann, Analysis Of Sound Patterns Through
561   Wavelet Transforms, International Journal of Pattern Recognition and Artificial
562   Intelligence. 01 (1987) 273–302, https://doi.org/10.1142/s0218001487000205.

563   [34]   T. Paul, Functions analytic on the half-plane as quantum mechanical states, Journal of
564   Mathematical Physics. 25 (1984) 3252–3263, https://doi.org/10.1063/1.526072.

565   [35]   J. Raja, B. Muralikrishnan, S. Fu, Recent advances in separation of roughness, waviness
566   and form, Precision Engineering. 26 (2002) 222–235, https://doi.org/10.1016/s0141-
567   6359(02)00103-4.

568   [36]   Y. Ge, H. Tang, M.A.M.E. Eldin, P. Chen, L. Wang, J. Wang, A Description for Rock Joint
569   Roughness Based on Terrestrial Laser Scanner and Image Analysis, Scientific Reports. 5
570   (2015), https://doi.org/10.1038/srep16999.

571   [37]   M. Bitenc, D.S. Kieffer, K. Khoshelham, Evaluation Of Wavelet Denoising Methods For
572   Small-Scale Joint Roughness Estimation Using Terrestrial Laser Scanning, ISPRS Annals
573   of Photogrammetry, Remote Sensing and Spatial Information Sciences. II-3/W5 (2015) 81–
574   88, https://doi.org/10.5194/isprsannals-ii-3-w5-81-2015.

575   [38]   K. Khoshelham, D. Altundag, Wavelet De-Noising of Terrestrial Laser Scanner Data for
576   the Characterization of Rock Surface Roughness, The International Archives of the
577   Photogrammetry, Remote Sensing and Spatial Information Sciences. 38 (1998) 373–378.
578   https://repository.tudelft.nl/islandora/object/uuid%3A520bf4ee-388c-4848-a8ec-
579   70eabcfafc50

580   [39] X. Chen, J. Raja, S. Simanapalli, Multi-Scale Analysis of Engineering Surfaces,
581   International Journal of Machine Tools and Manufacture. 35 (2) (1995) 231–238,
582   https://doi.org/10.1016/0890-6955(94)P2377-R

583   [40] B. Josso, D.R. Burton, M.J. Lalor, Frequency normalised wavelet transform for surface
584   roughness   analysis   and   characterisation,   Wear.   252   (2002)   491–500,
585   http://dx.doi.org/10.1016/s0043-1648(02)00006-6.

586   [41] K. Stępień, W. Makieła, An Analysis of Deviations of Cylindrical Surfaces with the Use of
587   Wavelet   Transform,   Metrology   and   Measurement   Systems.   20   (2013),
588   http://dx.doi.org/10.2478/mms-2013-0013.

589   [42] X. Jiang, L. Blunt, K. Stout, Lifting wavelet for three-dimensional surface analysis,
590   International Journal of Machine Tools and Manufacture. 41 (2001) 2163–2169,
591   http://dx.doi.org/10.1016/s0890-6955(01)00083-9.

592   [43] R. R. Coifman, M. Maggioni, Diffusion Wavelets, Applied and Computational Harmonic
593   Analysis. 21 (1) (2006) 53-94. doi: https://doi.org/10.1016/j.acha.2006.04.004

594   [44] H.S. Abdul-Rahman, X.J. Jiang, P.J. Scott, Freeform surface filtering using the lifting
595   wavelet   transform,   Precision   Engineering.   37   (2013)   187–202,
596   http://dx.doi.org/10.1016/j.precisioneng.2012.08.002.

597   [45] D. Mendlovic, N. Konforti, Optical realization of the wavelet transform for two-
598   dimensional   objects,   Applied   Optics.   32   (1993)   6542,
599   http://dx.doi.org/10.1364/ao.32.006542.

600   [46] V.V. Valenzuela, R.D. Lins, H.M.D. Oliveira, Application of Enhanced-2D-CWT in
601   Topographic Images for Mapping Landslide Risk Areas, Lecture Notes in Computer
602   Science Image Analysis and Recognition. (2013) 380–388, http://dx.doi.org/10.1007/978-
603   3-642-39094-4_43.

604   [47] R. Polikar, The Wavelet Tutorial. The Engineer's Ultimate Guide to Wavelet Analysis,
605   2006.

606   [48] P.S. Addison, The illustrated wavelet transform handbook: introductory theory and
607   applications in science, engineering medicine and finance, CRC Press, Boca Raton, 2017,
608   ISBN: 9781482251326

609   [49] I. Daubechies, Ten lectures on wavelets, Society for Industrial and Applied Mathematics,
610   Philadelphia, PA, 1992, https://doi.org/10.1137/1.9781611970104

611   [50] N. Wang, C. Lu, Two-Dimensional Continuous Wavelet Analysis and Its Application to
612   Meteorological Data, Journal of Atmospheric and Oceanic Technology. 27 (2010) 652–666,
613   http://dx.doi.org/10.1175/2009jtecha1338.1.

614   [51] J.-P. Antione, R. Murenzi, P. Vandergheynst, S. T. Ali, Two-dimensional wavelets and
615   their relatives, Cambridge University Press, Cambridge, 2008,
616   https://doi.org/10.1017/CBO9780511543395

617 [52] R. Leach, Characterisation of Areal Surface Texture, Springer Berlin, Berlin, 2013,
618 https://doi.org/10.1007/978-3-642-36458-7

619 [53] R.X. Gao, R. Yan, Wavelets - Theory and applications for manufacturing, Springer, New
620 York, 2011, https://doi.org/10.1007/978-1-4419-1545-0

621 [54] W.X. Yang, X.M. Ren, Detecting impulses in mechanical signals by wavelets, EURASIP
622 Journal on Applied Signal Processing. 2004 (2004) 1156-1162,
623 https://doi.org/10.1155/S1110865704311091

624 [55] D. Marr, E. Hildreth, Theory of Edge Detection, Proceedings of the Royal Society London.
625 Series B, Bioogical Sciences. 207 (1167) (1980) 187–217,
626 http://dx.doi.org/10.1098/rspb.1980.0020.

627 [56] J. P. Antoine, R. Murenzi, Two-dimensional directional wavelets and the scale-angle
628 representation, Signal Processing, 52 (3) (1996) 259–281, https://doi.org/10.1016/0165-
629 1684(96)00065-5.

630 [57] ACI Committee 117, ACI 117-10 Specification for Tolerances for Concrete Construction
631 and Materials and Commentary. 2010, ISBN: 9780870313790

632 [58] S. Kunis, Nonequispaced FFT: generalisation and inversion, Shaker, Aachen, 2007, ISBN
633 3832258787

634 [59] Leica Geosystems, Leica ScanStation P30/P40 product specifications, 2016. http://w3.leica-
635 geosystems.com/downloads123/hds/hds/general/brochures-
636 datasheet/Leica_ScanStation_P30-P40_Plant_DS_en.pdf

637